

# 3 Experiments and Methods

## 3.1 Dissociative Electron Attachment Spectroscopy in the gas phase

DEA reactions are studied by means of a crossed electron-molecular beams arrangement as it is shown in figure 3.1. The experimental setup is housed in a stainless steel high-vacuum (HV) chamber that is pumped by a turbo-molecular pump (Pfeiffer TMU 262 P) to a base pressure of  $10^{-8}$  mbar. A rotary vane pump (Alcatel 212A) supports the turbo-molecular pump; the pressure is measured by a Bayard-Alpert ion gauge (LH Ionivac IM 210D).

Powder samples are filled into a vessel and two halogen bulbs heat the whole chamber to moderate temperatures (50-100 °C) to prevent condensation of the molecules on the lenses and the walls of the chamber. The sublimated molecules are guided through a capillary to form an evaporative beam into the reaction zone where they collide with the monoenergetic electrons. The electron beam is generated by a trochoidal electron monochromator (TEM) [62]. The formed anions are mass selected by a quadrupole mass spectrometer (QMS) and detected by a secondary electron multiplier (SEM). In the measurements the mass spectrometer is set to a constant mass and the ion yield is recorded as a function of the electron energy.

A gas-inlet system (Swagelok) allows the introduction of the calibration gas or a sample with high vapour pressure through a leak valve into the high-vacuum

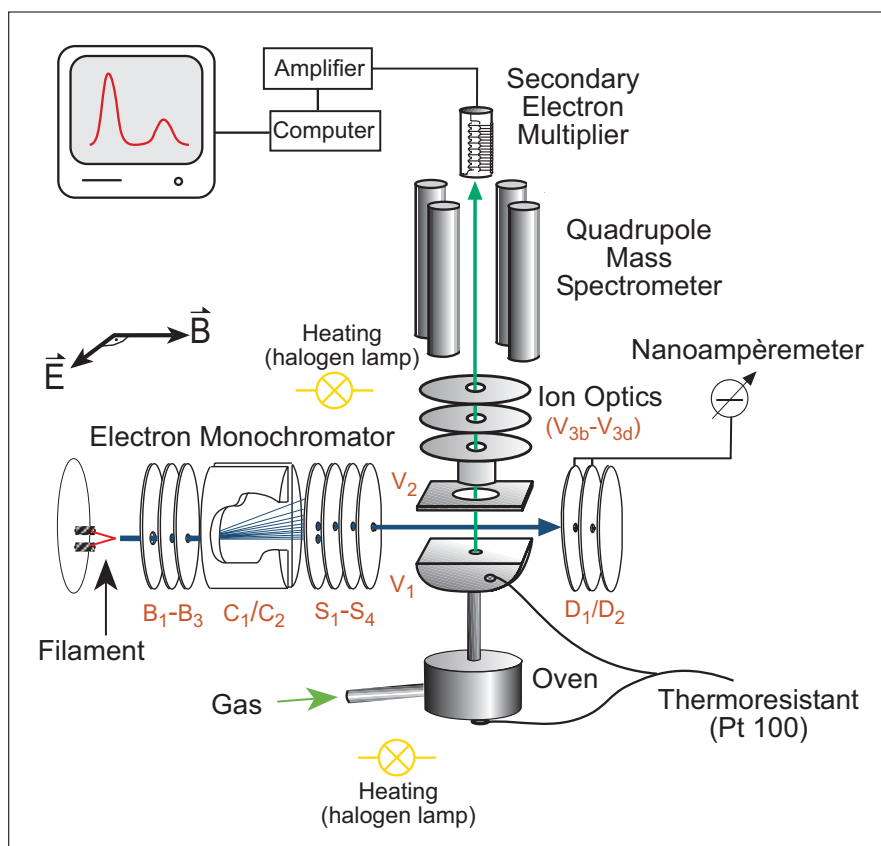


**Figure 3.1:** Scheme of the experimental setup used for dissociative electron attachment to gas phase molecules.

chamber. The gas-inlet system is equipped with an SF<sub>6</sub> gas cylinder and two additional connections for gaseous or liquid samples. The tubes are pumped by a rotary vane pump (Pfeiffer DUO 2.5A) and can be heated with a heating band.

### 3.1.1 Generation of the monoenergetic electron beam

The electrons are emitted from a hot tungsten filament that is supplied with a current of 2.3 A. A first series of three electrodes (B<sub>1</sub>-B<sub>3</sub>) with non-axial holes (figure 3.1) focuses the electrons into the dispersion region between two flat lenses (C<sub>1</sub>, C<sub>2</sub>), where the energy selection is accomplished. The C-lenses generate a homogeneous electric field similar to a parallel-plate capacitor. Due to an axial magnetic field the electrons are guided on trochoidal trajectories with the guiding

center moving in  $z$ -direction (perpendicular to the magnetic and the electric field). The magnetic field is generated externally by two Helmholtz coils. The deflection in  $z$ -direction ( $v_z$ ) depends on the strength of the electric field  $E$  and the magnetic field  $B$  according to [63]:

$$v_z = \frac{|\vec{E} \times \vec{B}|}{B^2} \quad (3.1)$$

The next lens ( $S_1$ ) possesses an axial hole and collects all electrons having a certain velocity and thus a corresponding deflection in  $z$ -direction. The displacement  $D$  between the axial holes of the B-lenses and the non-axial holes of the S-lenses strongly influences the energy spread  $\Delta\omega$  of the electron beam [63] according to:

$$\Delta\omega = \frac{E^2 L^2 m \Delta D}{B^2 D^3} + eEb_3 \quad (3.2)$$

$L$  denotes the length of the dispersion region and  $\Delta D$  the sum of the aperture diameter of the entrance and exit apertures ( $b_3 + s_1$ ). The magnetic field  $B$  is around 100 Gauss (10 mT). For the present configuration ( $E_{min} = 100$  V/m,  $L = 19.8$  mm,  $\Delta D = 2.8$  mm,  $D = 2.2$  mm,  $b_3 = 1.2$  mm) a limit for the full electron energy spread can be estimated to be  $\Delta\omega = 142$  meV. The energy resolution is assumed to be the full-width at half maximum (FWHM; see next section) of the calibration gas and for the TEM the  $FWHM \approx \Delta\omega/3$  [63], resulting in a maximum resolution of  $\approx 50$  meV. During experiments the resolution of the electron beam can be controlled by changing the relative potentials of  $C_1$  and  $C_2$  and hence the electric field  $E$ .

The set of S-lenses ( $S_1 - S_4$ ) refocusses and accelerates or decelerates, respectively, the monoenergetic electrons into the reaction zone, where they interact with the effusive molecular beam. Transmitted electrons are collected behind the reaction chamber by two additional lenses ( $D_1, D_2$ ). The current is measured at these two lenses and is usually 10-20 nA. All electrodes are made of 1.5 mm thick molybdenum plates, which are isolated from each other by ruby balls.

### 3.1.2 Calibration of the energy scale

The energy scale is calibrated using SF<sub>6</sub> that forms metastable SF<sub>6</sub><sup>-</sup> by s-wave electron capture very close to 0 eV electron energy. The width of the resonance was determined previously to be below 1 meV [34, 38]. Thus the observed full-width at half maximum (FWHM) of the SF<sub>6</sub><sup>-</sup> signal in the present experiment is only limited by the resolution of the electron beam. Hence the FWHM is used as a means to determine the electron energy resolution that is usually in the range 90-150 meV in the present experiments.

The cross section of SF<sub>6</sub><sup>-</sup> formation is very large (2.57×10<sup>-18</sup> m<sup>2</sup> at 25 meV [64]) and thus about two orders of magnitude larger than the geometrical cross section of the SF<sub>6</sub> molecule (≈7.6×10<sup>-20</sup> m<sup>2</sup>). A mean value of 2.4×10<sup>-18</sup> m<sup>2</sup> can be calculated from the rate constant of thermal electron attachment (k=3.1×10<sup>-7</sup> cm<sup>3</sup>s<sup>-1</sup> [65]) and the mean velocity of the electrons at 300 K ( $\bar{v}$  = 1.2×10<sup>7</sup> cm/s [28]) using equation 2.19. The attachment cross section rises closer to 0 eV to even higher values (7.6×10<sup>-17</sup> m<sup>2</sup> at 0.1 meV [64]), but it depends on the quality of the electron beam which low-energy values can be reached.

In the present experiments an absolute cross section for DEA into a fragment A<sup>-</sup> can be estimated by comparison of the A<sup>-</sup> ion yield and partial pressure of the target molecule generating A<sup>-</sup> with the SF<sub>6</sub><sup>-</sup> ion yield and the SF<sub>6</sub> partial pressure:

$$\left(\frac{\sigma_A}{\sigma_{\text{SF}_6}}\right)_{0\text{eV}} = \left(\frac{S_A}{S_{\text{SF}_6}}\right)_{0\text{eV}} \times \left(\frac{\rho_{\text{SF}_6}}{\rho_A}\right)_{0\text{eV}} \quad (3.3)$$

There are two main sources for uncertainties: 1. The actual pressure in the effusive beam is not exactly known, on the other hand it is assumed that the pressure difference between ion gauge and reaction zone is the same for SF<sub>6</sub> and the sample molecules. 2. The ion gauge is not calibrated for the different ionisation cross sections of SF<sub>6</sub> and the sample molecules. Therefore the absolute cross section can only be estimated within one order of magnitude.

### 3.1.3 Ion detection

In the reaction zone a weak electrical field in the order of 1 V/cm, generated by the electrodes  $V_1$  and  $V_2$ , guides the formed anions into the ion optics ( $V_{3b}$ - $V_{3d}$ ) of the quadrupole mass spectrometer (Balzers QMG 311).

The rods of the QMS are supplied with a superposition of alternating voltage (amplitude  $V$ ) and direct voltage ( $U$ ) creating an alternating electric quadrupole field that guides the ions on oscillating trajectories. Depending on the  $U/V$  ratio only ions with a certain mass to charge ratio follow stable trajectories. All other ions hit the rods and get neutralised. The flight-time of an ion through the quadrupole is approximately  $50 \mu\text{s}$ . Ions that further decompose within the QMS are not detected as well.

The transmitted negative ions are collected by the conversion dynode of a secondary electron multiplier (SEM) that is set to a positive voltage. The SEM consists of 17 Cu/Be dynodes, that are supplied with an overall voltage of 3.6 kV. By subsequent secondary-electron emission and acceleration to the respective next dynode an electron pulse is generated at the collector. The final pulse is decoupled to ground level by a blocking capacitor, amplified by a preamplifier and then transformed into a TTL pulse by a single-channel analyser. The TTL pulse is read by a PCI card of a personal computer and displayed as ion count rate by a LabView program.

## 3.2 DEA Spectroscopy using Laser Induced Acoustic Desorption (LIAD)

### 3.2.1 The experimental setup

A scheme of the new experimental setup is presented in figure 3.2. A stainless steel vacuum chamber is pumped by a turbo pump (Pfeiffer TPU 330), which is supported by a rotary vane pump (Pfeiffer DUO 012A). The background pressure is measured by a cold cathode gauge (Balzers IKR 250) and amounts to  $10^{-7}$  mbar. The electron gun consists of a tungsten filament in a Wehnelt cylinder-

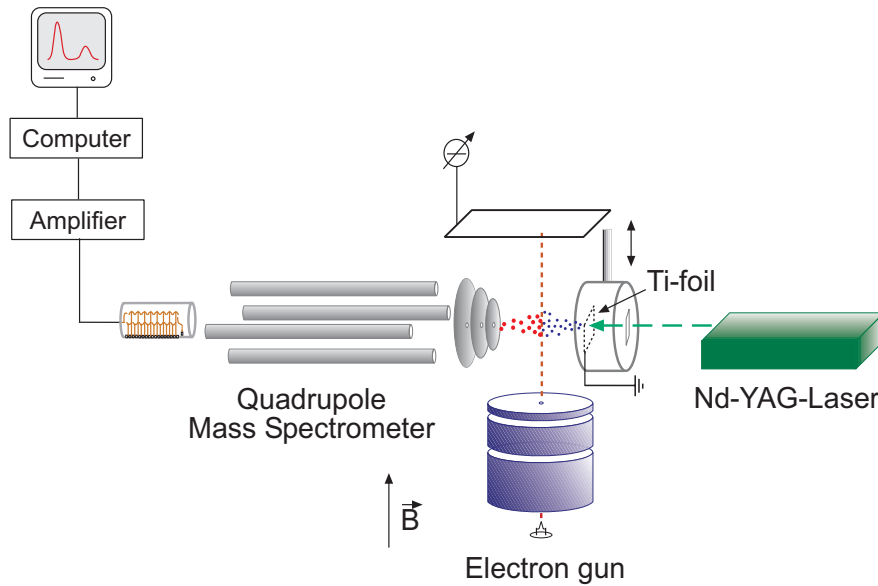


**Figure 3.2:** Experimental setup LIAD.

der and three additional molybdenum lenses. To align the electrons an external magnetic field is applied by means of two Helmholtz coils.

For each coil 20 m of magnet wire is wound on an aluminum carrier and hold by two circular slabs having a diameter of 40 cm. To provide a homogeneous magnetic field inside the chamber the distance between the Helmholtz coils are supposed to match the radius of the coils. The magnetic field  $B$  of this arrangement

can be calculated by the following expression that is derived from the Biot-Savart equation [66]:

$$B = \frac{N\mu_0 8I}{\sqrt{125}R} \quad (3.4)$$

with  $N$  the number of turns,  $\mu_0$  the magnetic field constant,  $I$  the supplied current and  $R$  the radius of the coils. For the present experimental setup ( $N=1700$ ,  $I=3.5$  A,  $R=35$  cm) the magnetic field is  $\approx 150$  Gauss (15 mT).

The electron current is 2-3  $\mu$ A and is measured by a simple molybdenum plate behind the reaction volume. If the current is too high, the space charge prevents an acceptable resolution at low electron energies, thus the maximum emission current applied through the filament is 2.1 A. The energy resolution is 0.6 to 1.2 eV. The energy scale is calibrated using the formation of metastable  $SF_6^-$  as was described above.

The generated anions are focused into the quadrupole mass spectrometer by ion optics consisting of three lenses. The QMS is arranged perpendicular to the electron beam and opposite to the Ti foil with a distance of approximately 1 cm. Mass selected ions are detected by a SEM, the generated pulse is amplified by a preamplifier, converted into a digital signal and read by a PCI card (National Instruments, PCI-6221) of a personal computer. Mass spectra and DEA spectra are recorded using software written in LabView that also controls the electron energy.

A gaseous sample can be introduced through a gas-inlet system with a leak valve and a capillary directing into the reaction volume.

The performance of the electron beam was tested and optimised by means of  $SF_6$ . The 0 eV resonance generating  $SF_6^-$  was used to improve the ion yield and the energy resolution. At higher energies (5-12 eV) electron attachment to  $SF_6$  creates  $F^-$  with maxima at 5.7, 9.3 and 11.8 eV. In figure 3.3 the  $SF_6^-$  and  $F^-$  ion yields are displayed to demonstrate that the electron gun can be used in the low energy region 0-10 eV.

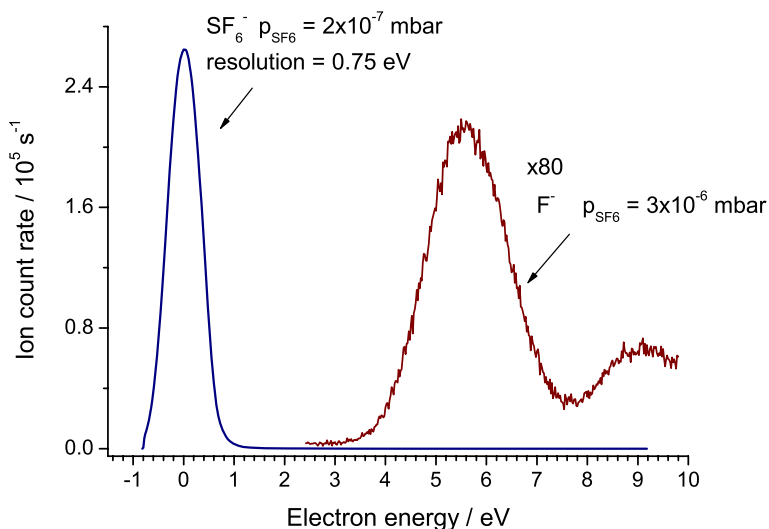


**Figure 3.3:**  $\text{SF}_6^-$  and  $\text{F}^-$  ion yield following electron attachment to  $\text{SF}_6$ .

### 3.2.2 The sample holder

The sample must be moved with respect to the laser beam in order to irradiate different spots, since the sample molecules can be removed completely after a certain number of laser shots. It is advantageous to move the sample holder rather than the laser beam as the same optimised conditions can be maintained during the measurements.

In figure 3.4 a scheme of the sample holder and the laser feedthrough is shown. Both are connected to different flanges. The sample holder itself is made from Kel-F and carries the Ti foil (15 x 15 x 0.013 mm) along with a glass slide which is used as protection for the quartz window against sputtered Ti. The glass slide is replaced after each measurement. The sample holder is movable in one direction by means of a micrometer screw.

The laser light is coupled into an optical fibre (600  $\mu\text{m}$  core diameter). Two bifocal lenses focus the light onto a spot of the size  $5 \times 10^{-3} \text{ cm}^2$ . A quartz window separates the vacuum chamber from the atmosphere. In the present experiments the second harmonic of a pulsed Nd:YAG laser (532 nm) is used (Minilite I,



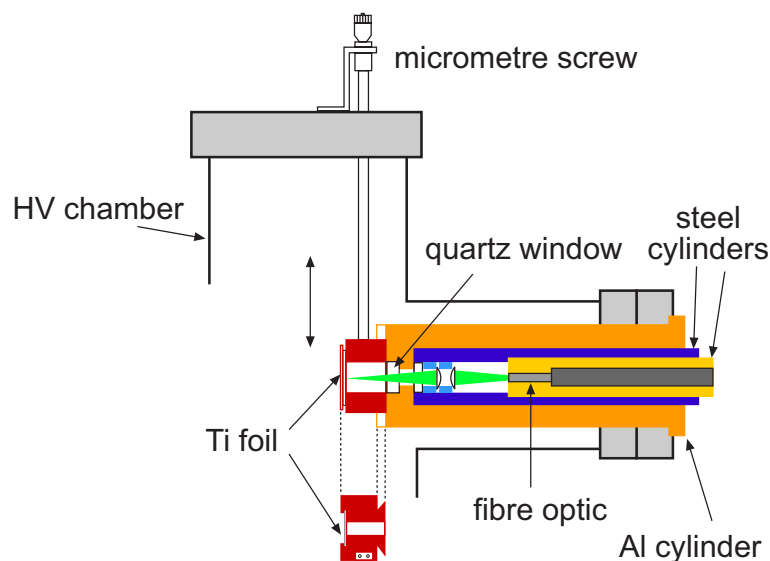


**Figure 3.4:** The sample holder and laser feedthrough. The quartz window separates the vacuum from atmosphere.

Continuum). The energy per pulse is 3 mJ with a pulse duration of 2-6 ns.

The fibre optic is held by a steel cylinder that can be moved in one direction within a second, outer cylinder. The outer cylinder is also movable in order to exactly focus the laser light onto the Ti foil.

### 3.2.3 Laser desorption

Two conditions must be fulfilled in the new setup: 1. The desorption process must be effective in order to have sufficient particle density in the interaction region with the electrons and eventually an adequate ion signal, 2. The ion signal must be maintained over a relatively long time, i.e. up to several minutes to be able to perform mass scans with the QMS or electron energy scans at a fixed mass, respectively.

To characterise the laser desorption process the red dye Rhodamin 6G was used as sample and the laser was focused on the backside of the foil outside the vacuum chamber. A continuous He-Ne laser was placed perpendicular to the Nd:YAG laser in front of the foil in order to observe scattered light from desorbed particles.

It was observed that after a few shots a maximum of the scattered light was reached and maintained for several minutes. Afterwards the irradiated spot was blank indicating that all molecules were desorbed. By changing the distance of the He-Ne laser with respect to the surface of the foil the distance of desorbed particles could be estimated. It was found that the travel length of particles exceeds 8 mm.

#### 3.2.4 Sample preparation

All samples used here (5-bromouracil, thymidine and 5-ribosephosphate) were dissolved in Methanol. Approximately 0.1 ml of a 0.1 M solution are deposited on the Ti foil and the solvent is removed quickly at low pressure to form a homogeneous layer of sample molecules.

The area of one Ti foil is  $\approx 225 \text{ mm}^2$ , and the size of the laser spot is about  $1 \text{ mm}^2$ . If  $10 \mu\text{mol}$  of the sample are deposited on the entire foil,  $\approx 50 \text{ nmol}$  are desorbed from one spot, if all molecules are completely removed. Assuming a reaction volume of  $1 \text{ cm}^3$  the maximum particle density is thus  $\approx 10^{16}$  molecules per  $\text{cm}^3$ .

### 3.3 Matrix-Assisted Laser Desorption/Ionisation (MALDI)

The MALDI experiments (see chapter 4.1.3 on page 58) have been performed at the University of Iceland with a REFLEX IV (Bruker Daltonics) UV-MALDI-Time-of-flight (TOF) reflectron type instrument (figure 3.5). It is equipped with an N<sub>2</sub> laser (337 nm, 400 μJ/pulse) operated with 7-10 Hz repetition rate.

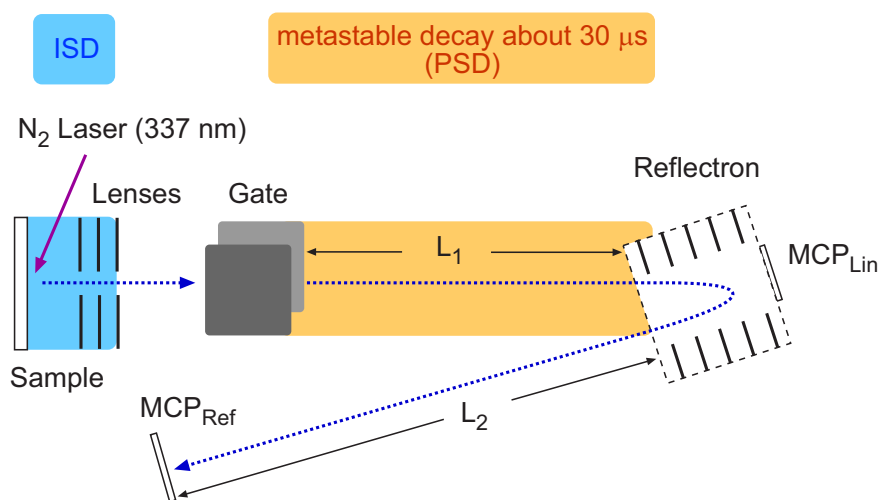


**Figure 3.5:** Scheme of the MALDI experiment. In post-source decay (PSD) the fragmentation of a selected ion within the first drift tube (L<sub>1</sub>) is measured by reaccelerating the fragment ions into the second drift tube (L<sub>2</sub>).

Ions generated by the laser pulse are extracted by a pulsed high voltage of +25 kV with a delay time of 400 ns. Thus the ions gain the kinetic energy  $z \cdot e \cdot U$  and are then entering a field free tube. The flight time depends on the mass according to:

$$t = \Delta x (m/2zeU)^{1/2} \quad (3.5)$$

The instrument can be operated in linear mode, i.e. the ions are detected after the linear flight, or in reflectron mode. In the latter case the ions

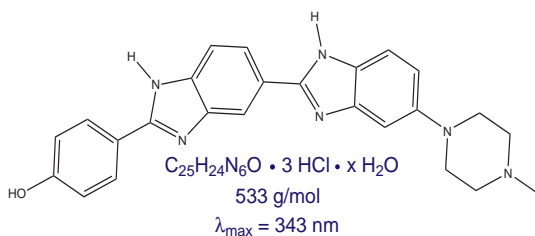


**Figure 3.6:** Molecular structure of bisbenzimidazole.

which are due to varying initial kinetic energies.

In measurements of metastable decay a certain mass is selected at a gate, that is located at the beginning of the first drift tube. The gate blocks all ions and is opened for a small time window to let a certain group of ions pass (for the present experiments an accuracy of  $\pm 2$  amu was employed). The decomposition of the selected ion within the first flight tube ( $L_1$ ) is analysed by reaccelerating the fragment ions at the reflectron and detecting them after the second drift tube ( $L_2$ ).

As matrix bis-benzimidazole was used (figure 3.6) as its absorption maximum lies at 343 nm and the molecular mass (424 amu) is higher than the masses of the sugars studied here to minimise disturbing signals in the spectra. Samples were prepared by deposition of  $0.5 \mu\text{L}$  of a 3.5 mM solution of matrix in methanol on a stainless steel sample carrier and allowed to dry in air. Afterwards  $0.5 \mu\text{L}$  of 0.13 M D-ribose or D-fructose solution, respectively, was spotted on the matrix and allowed to dry.

are decelerated at the end of the linear flight by an ion mirror and reflected into a second field free drift tube and finally recorded on a micro channel plate detector. This procedure increases the mass resolution since differences in flight time are suppressed,

## 3.4 Calculations

To evaluate thermodynamic thresholds and possible structures of stable fragment anions density-functional theory (DFT) calculations have been performed on D-ribose and two representative fragment anions (chapter 4.1.2). All geometries have been optimised using the B3LYP functional and 6-31++G\*\* basis set. Thermodynamic thresholds were determined by calculating the difference between total electronic energies of D-ribose and the anionic and neutral fragments. Adiabatic electron affinities of fragment anions were calculated from the difference of neutral and anionic electronic energies. The reported energies have been corrected for zero-point vibrational energies (ZPE). All calculations have been performed with Gaussian03 [67].

